



WING CELL GEOMETRY AND PRESSURE DISTRIBUTION OVER THE SURFACE OF A PARAGLIDER

Md. Mahfuz Sarwar and Mohammad Mashud

Department of Mechanical Engineering

Khulna University of Engineering & Technology (KUET)

Khulna-9203, Bangladesh

E-mail: mahfuzsarwar@yahoo.com

Received Date: 18 June 2010; Accepted Date: 31 July 2010

Abstract

The paraglider poses an interesting challenge to the aerodynamics researcher. This paper studies aerodynamic issues involved in the deployment and operation of a paraglider. The surface shape of the paraglider is determined by the pressure distribution in and around the paraglider, the porosity of the fabric, and the presence of cell cross-flow, in addition to the fabric structure and the tensions in the lines at the attachment points. In this studies wind tunnel test of a three dimensional paraglider wing canopy cell model has been performed. Two dimensional (i.e. pressure measurement along the cord length and span wise direction) pressure distributions over the surface have been investigated at different angle of attack, simultaneously wing surface shape profiles has been measured directly. Surface contours of paraglider during operation in a wind tunnel are obtained. The pressure distribution in turn depends on the attitude and the surface shape. It has been observed that the minimum pressure over the surface of the wing increases towards the edges from the central section. Wing end effects also been investigated. There are a certain percentage of upper surfaces affected by the downwash.

Keywords: Paraglider, Aerodynamics, Flexible wing, Three dimensional measurements.

1. Introduction

The paraglider wing is currently under study as a controllable lifting device for landing space vehicles. It has also been suggested for other applications such as recovering rocket boosters and effecting reentry into the earth's atmosphere. Paraglider-load-systems are unique devices for recovery, rescue and delivery of air cargo [10]. The NASA X-38 Experimental Crew Recovery Vehicle uses a paraglider during the final stage of the landing approach. Various wind-tunnel and free-flight investigations have been made using either flexible or rigid idealizations of paraglider wings in order to find stability and control characteristics or shape analysis [1-4]. Ware and Hassell [5] conducted tests of tethered paraglider at the low speed wind tunnel. The models were double membrane wings with rectangular plan forms and airfoil cross-sections with open leading edges. Goodrick [6, 7] developed an analysis of static and dynamic longitudinal stability of high-performance gliding airdrop systems. He showed that for heavy payloads, the influence of canopy air mass may cause significant adverse dynamics. Goodrick extended the work of simulation, and discussed scale effects evident from experimental data, on tilt and turn rates. Brown [8] studied testing techniques to measure the performance of full-scale paraglider. C. Matos et al [9] measured the section profiles and leading-edge collapse of a paraglider during operation in a wind tunnel based on video photogrammetry combined with a laser sheet. None of the investigations of the three dimensional measurement, surface contour and pressure distribution on the flexible surface of the present shape paraglider wing has been done. In

our previous paper [11] we had discussed the one dimensional for pressure distributions and two dimensional measurements for surface profiles of flexible wing. As the surface of the paraglider is not flat, the three dimensional measurement will show the better result than two dimensional measurement. In our previous work we had performed the pressure and profile measurements at the central line on the surface of the wing along the chord line. In this paper two dimensional for pressure distributions and three dimensional for surface profiles measurement's, i.e. along the chord as well as along the span, results will be discussed.

2. Experimental Procedure

One cell model of a paraglider wing canopy was tested by the wind tunnel of 1360 cm² test section at Nagoya University, Aerodynamics and Propulsion Laboratory. The experimental set-up and procedure are same as our previous work [11] but the model preparation technique is little bit different than the previous model [11]. For the convenience of marking the measuring points on the inflated surface, we have drawn 29 and 77 parallel lines along the transverse and longitudinal direction on the surface of the soft cloth, respectively, before wrapping along the perimeter of the rigid ribs. The usual paraglider wing canopy is free from wing tip vortex/three dimensional effect due to the curvature along the span of the wing canopy. As we made only one cell model, certainly the both sides of the model will be affected by wing tip vortex. Two pieces of acrylic sheets, each sheet size 500mm×500mm, are attached on the both ends (sides) of the model to avoid the wing tip vortex/three dimensional effect.

3. Results and Discussions

3.1. Inflated wing shape

C. Matos et al [9] used Video-based photogrammetry method combined with a laser sheet to measure the section profiles of a paraglider wing cell model. In this studies we have measured the inflated surface coordinates directly by using the same pressure probe tip which was used to measure the surface pressure. Through the surface geometry results, the attack angles α of the paraglider wing cell model was 0° to 30°, and measured from leading edge to trailing edge & span wise (wing's one side to another side) . The paraglider wing cell model shows less curvature on the back half of the chord line than the front half. All measurements were conducted in such a way that the model inflates into a stable shape without any appreciable fluctuations of the vinyl cloth. Fig. 1 shows the measured shape of inflated cell model at various attack angles.

As shown in Fig. 1, it is found that at zero attack angle α leading edge collapse/deformation begins from the central/middle section of the upper surface of the paraglider cell model, more of the leading edge collapses at the central section and the collapse decreased outwards along the span. Due to the leading edge deformation the lip of the upper and lower surfaces become closer to each other, resulting in a small opening of air intake. As more of the leading edge collapses, the effective air intake height decreases further. If the air intake height becomes too small, the air intake no longer covers the range of movement of the stagnation streamline. Consequently, the stagnation point moves onto the upper surface of the lip. Due to the movement of the stagnation point onto the upper surface of the lip, increased the pressure on the deformed leading edge surface and the net pressure force acting on the deformed portion of the upper surface is partially balanced by the tensile force of the surface which is connected to the rigid ribs. The ribs of the model cell could not keep the airfoil shape if they were made of soft clothes because the membrane force tends to compress the leading part of the ribs.

The shape of the inflated cell model changes drastically when the attack angle α increased slowly by small increments. The leading part of the upper surface suddenly moves upward and forth, as a result there was no longer deformed/dented portion in front of the cell model as well as the effective air intake height increases. This implies that the stagnation point moves to a point located ahead of the air intake. A further increase in attack angle α larger than two degrees makes no significant change of air intake size and overall inflated wing shape, only orientation changed. In all cases of attack angle α ranging from 2 to 30 degrees, the inflated surface position is above to the rib of the wing. At 2, 4 and 6 degrees attack angles α , the rear portion (near to trailing edge) of the paraglider cell model surface seems to be flat along the span. And at 8, 10 and 15 attack angles α , the inflated surface near the trailing edge inflates more than the others attack angle α , that is, the inflated surface makes large curvature due to maintaining high inner pressure of the cell model. For this large curvature of the inflated surface fluid flows smoothly over the surface with small pressure gradient .

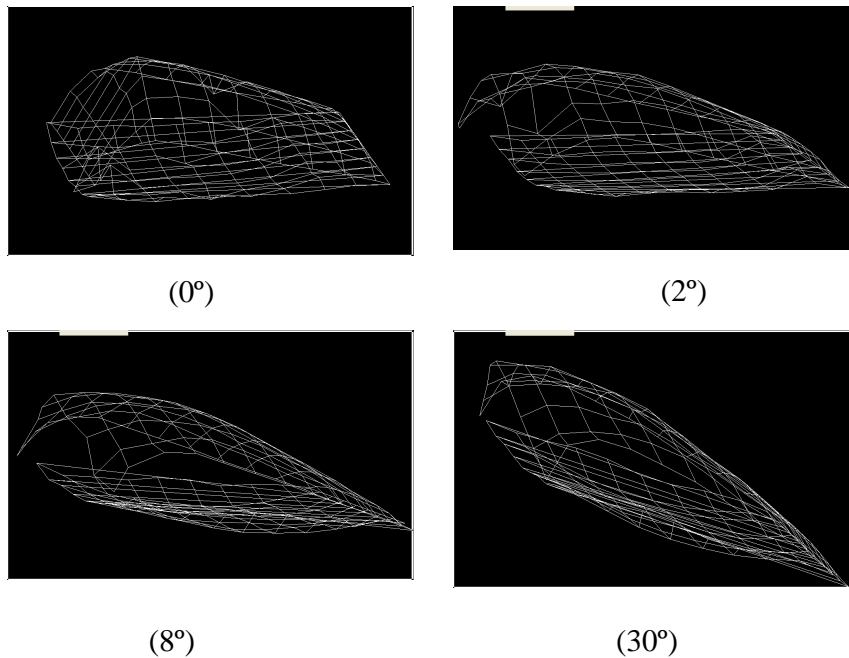


Fig.1. Wing shape at different attack angles.

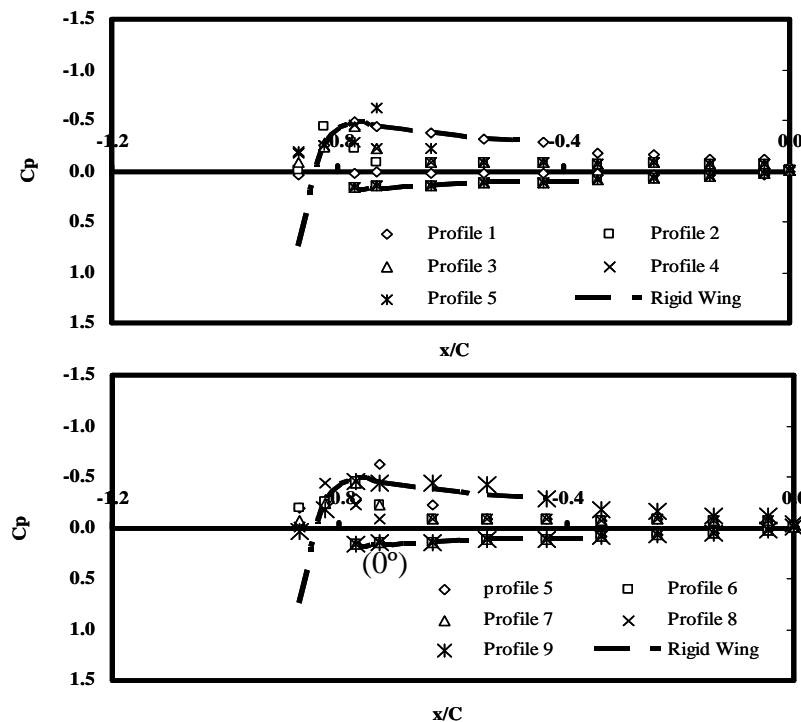
At the higher attack angles α a small portion, near the central line region, of the upper leading edge shows like flat. There is no pressure gradient at this region which is also observed in upper surface pressure distributions. As the leading edge is free from other forces than tensile force acting along their edge lines so it could make smallest radius of curvature. It has also been observed, wrinkle generates far away from the central line and near to ribs, which starts from the leading edge and diagonally goes toward the trailing edge up to 40% (about) of the chord length afterward disappear. Wrinkle generates from the leading edges near to ribs because the sides (leading edge) of the inflatable material are fixed with rigid ribs and during inflation of the upper surface the free leading edge moves/displace towards the trailing edge as well as towards up from its original position (attack angle α must be greater than zero) but the edges couldn't move and consequently maximum tensile force acts on the wrinkle line.

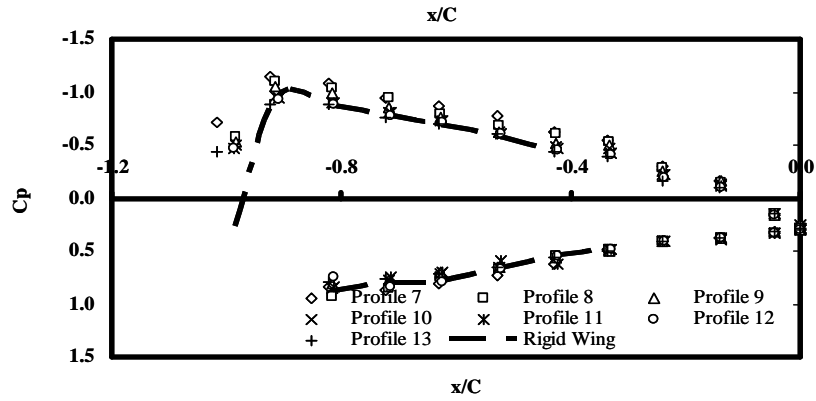
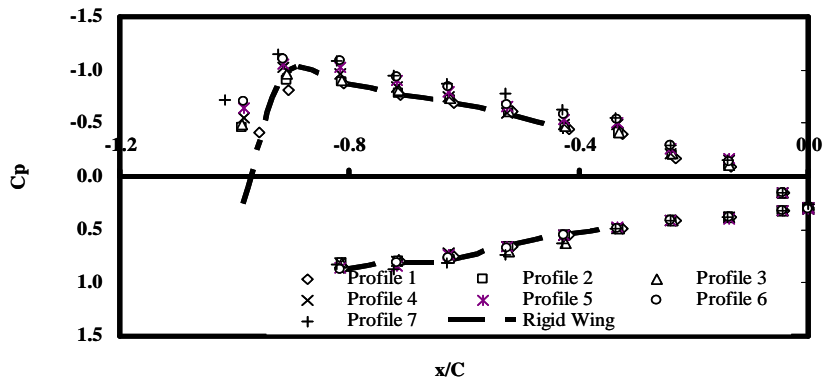
3.2. External surface pressure distribution

In this studies external pressure on the inflated surface of the cell model has been measured both along the chord line from leading edge to trailing edge and along the span from one end to another end over the pre-marked point at different attack angles α . There are no significant changes of the external surface pressure distributions for different Reynolds Number [11], that's why we have studied only one Reynolds Number for this paper. The pressure distribution results are discussed below

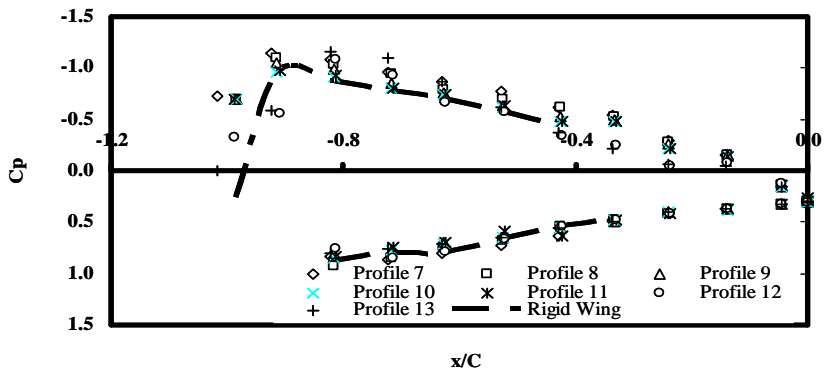
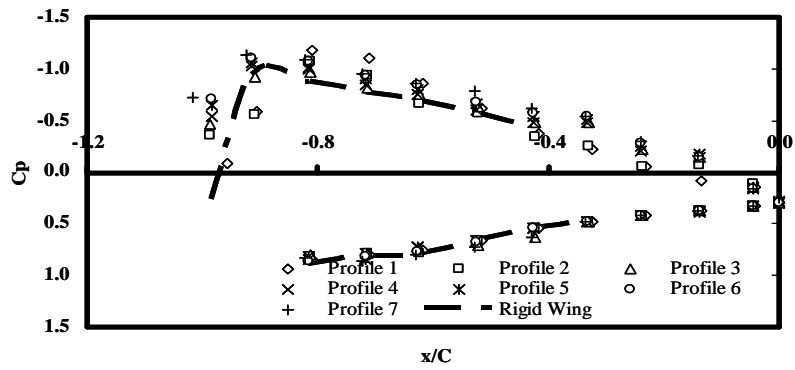
3.2.1. External surface pressure along the chord

As shown in Fig. 2, the upper and lower surface pressure distributions are presented as a plot of upper surface pressure coefficient C_{pU} and lower surface pressure coefficient C_{pL} fraction of local chord projected to the plane of the leading edge and total chord length (dimensionless distance x/C). And considering the profiles, fraction of local span projected to the plane of the model ends (ribs) and total span length. Profile 1 ($x/S=0.0$) begins from one rigid rib position (end) and profile 7 ($x/S=0.5$) represent the central line of the span. It is found that at zero attack angle the upper and lower surface pressures are almost equal (close to the ambient air pressure) except the deformed portion on the upper surface, that happens due to the separation of the main stream flow at the beginning of the inflated leading edge of the upper surface, because the stagnation point of the uniform stream is located on the deformed portion of the upper sheet. As the attack angle α increased by small increment (from zero to two degrees) the stagnation point moves to the in front of air intake from the upper surface (deformed upper leading edge) and consequently there is no any more deformed portion on the upper surface of the cell model as well as cell model inflates fully and get the real shape of the wing. At 2 to 8 degree attack angles α , when the stagnation point is located ahead of the air intake the separated flow region is restricted to a vicinity of the leading edge of either upper or lower surface. As the attack angle increases stagnation point moves toward the leading edge of the lower surface and the external pressure on the lower surface increases. On the other hand, the velocity of fluid turning the apex of the upper surface increases, resulting in a large magnitude of negative pressure there.





(8° with side plate)



(8° without side plate)

Fig. 2 Pressure distributions at different attack angles and profiles (Cont'd)

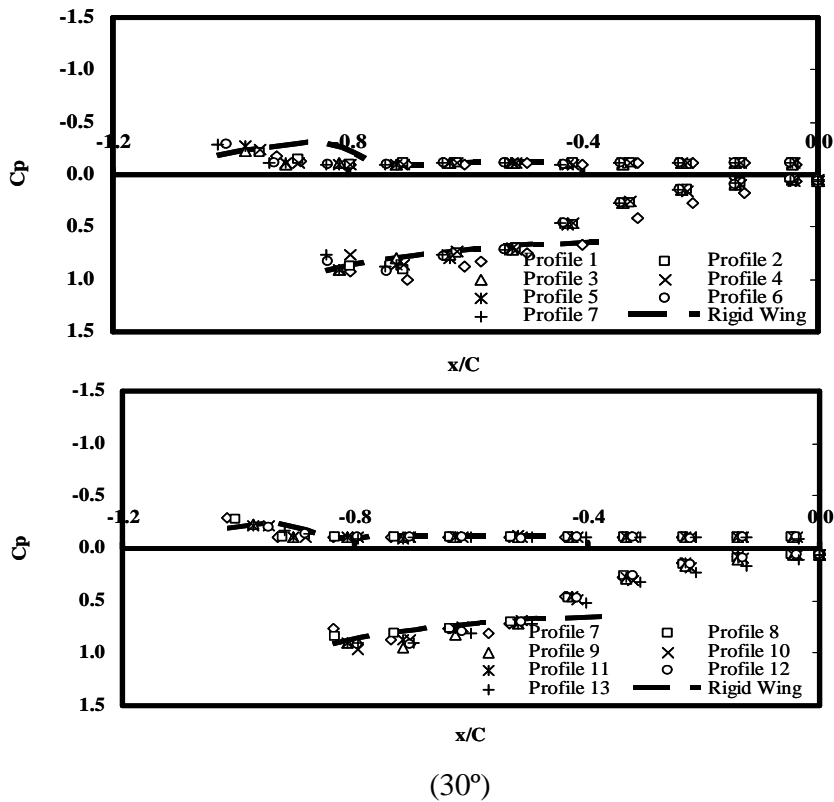


Fig. 2. Pressure distributions at different attack angles and profiles

The abrupt changes in the upper surface pressure is due to a kink of the upper surface profile caused by the three dimensional geometrical and dynamical construction of the sheet. As the attack angle α further increases to 15 degree, start to generate the separation bubbles on the upper surface at the rear portion of the cell model because the fluid is no longer able to follow the contour of the curved surface and it separates from the surface. At 20 degree attack angle α , the upper surface down stream flow appears a clear separation zone which was about 25% area of the upper surface just before the trailing edge. At 30 degree attack angle α , the value of pressure coefficients (near about zero) is almost unchanged along the upper surface just after the leading edge. At large attack angles α , the leading edge pressure coefficients of the lower surface are almost equal to unity and greater than the internal pressure coefficient there. Therefore, this part is pushed inward by the internal air. However, since the leading edge is located upside and downstream of the leading edge of the lower perimeter of the rigid rib, this part is pulled by the rib similarly to the leading edge of the upper sheet.

3.2.1 External surface pressure along the span

Fig. 2 shows the pressure distributions on the upper and lower inflated surfaces of the cell model along the chord against the dimensionless distance x/C and different profiles along the span at various attack angles α . From Fig. 2 it has been seen that the lower surface pressure distribution along the span is almost equal for each attack angle α , as the radius of curvature of the inflated lower surface is too large (tends to infinity) so the pressure gradient of the neighbors measuring points along the span are negligible amount, but the pressure along the chord gradually increases from the leading to trailing

edge due to the shape of the wing model. It is found that at the attack angle α ranges 2 to 20 degree, for upper inflated surface pressure distribution, the minimum pressures appear along the central line of the wing model except the rear portion of the cell model. The radius of curvature of the upper inflated surface gradually increases from leading edge to trailing edge and nearer to trailing edge the inflated surface is almost flat due to model construction technique (the inflated cloth was tapered toward both ends so that the leading parts of the upper and lower surfaces have freedom to deform when the cell model inflates. The narrowest part of the cloth was attached to the trailing edges of the ribs, and its width was taken equal to the distance between the rigid ribs). Pressure increases on the each and every point towards the edges from the central line of the cell model, as the height of the air intake is maximum at the center and minimum on the edges so the velocity gradient is higher at the center on the upper inflated surface than edges. At 8 degree attack angle α , the variation of magnitude of negative peak pressure coefficient between the central line and the edges of the wing is about 0.2 for the wing thickness difference 12%, which is consistent with NACA's airfoil data. Differences of negative peak pressure coefficient between NACA 2430 and NACA 2418 airfoil is about 0.15 at the same attack angle α (8 degree). At 0 and 30 degrees attack angle, the main stream flow is fully separated on the upper surface from the beginning of leading edge that means stable flight is impossible at these attack angles.

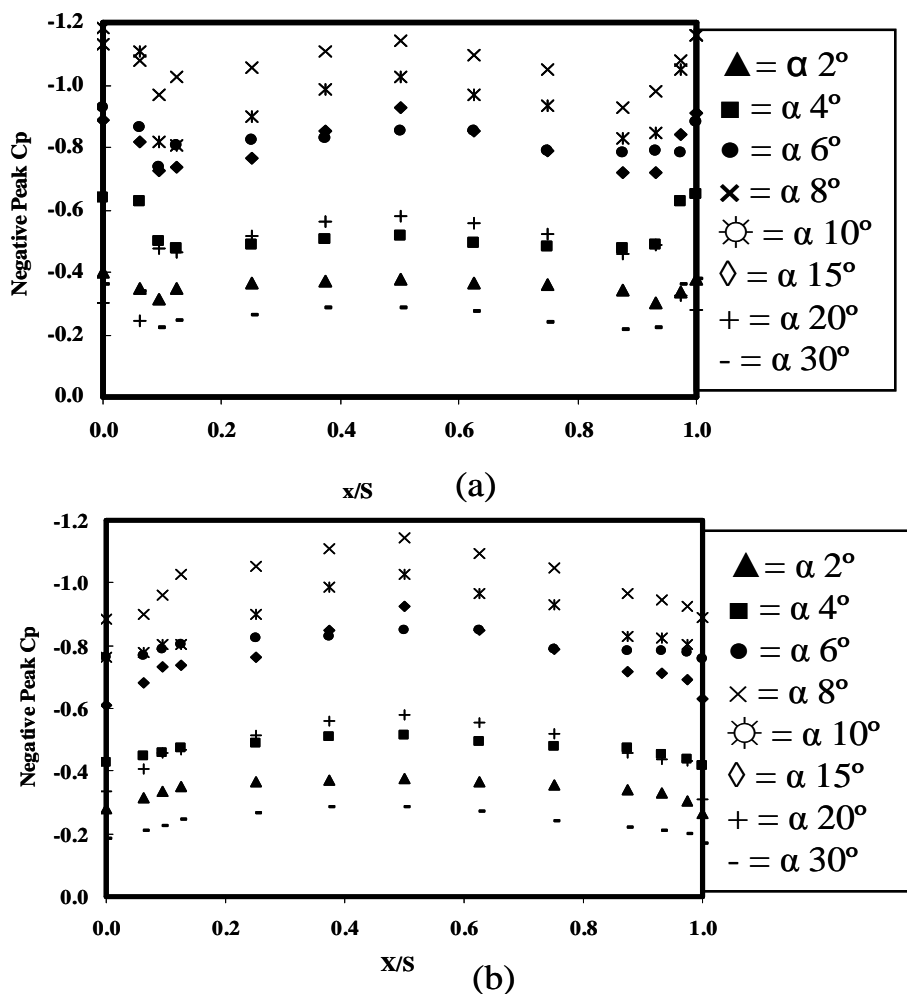


Fig. 3. Negative peak pressure coefficients along the span, (a) without side plate and (b) with side plate

Negative peak pressure coefficients (C_{pUmin}) of upper surface are shown in Fig. 3 at different attack angles α excluding and including side effect. As shown in Fig. 3(a) we can see that the upper surface pressure gradually increases towards the edges, from the central section, of the wing but suddenly starts to fall down near to edges of the wing. If the wing has lift, then obviously the average pressure on the lower surface is greater than that on the upper surface. Consequently, there is some tendency for the air to leak or flow, around the wing ends from the high to the low-pressure sides. This flow establishes a circulatory motion which ends downstream of the wing. This downstream induces a small velocity component in the downward direction at the wing. Due to this effect increases the local flow velocity in vicinity of wing but changes the direction of flow as well as decreases the pressure gradient. In this observation, it is found; about 15% wing's ends area on the upper surface are affected by downwash/wingtip vortex. This percentile may vary for different model size.

4. Conclusions

Three dimensional measurements for inflated wing shape and aerodynamic properties of paraglider's canopy were tested in the wind tunnel experiment using the inflatable cell model. Fully inflated and stable airfoil shape model has been found at an attack angle greater than zero. In this study, we have concentrated the attention to the three-dimensional shape of the inflated cell model and external surface pressure distribution all over the inflated surface at different attack angle. The average lift coefficient of this measurement is slightly less than two dimensional measurement's result but the lift to drag ratio is greater than that one.

References

- [1] F. M. Rogallo, J. G. Lowry, D. R. Croom, and R.T. Taylor, "Preliminary Investigation of a Paraglider," *NASA TN D-443*, 1960.
- [2] D. E. Hewes, "Free-Flight Investigation of Radio-Controlled Models with Parawing," *NASA TN D-927*, 1961.
- [3] P.G. Fournier and B.A. Bell, "Low Subsonic Pressure Distributions on Three Rigid Wings Simulating Paragliders With Varied Canopy Curvatures and Leading-Edge Sweep," *NASA TN D-983*, 1961.
- [3] B. Gamse, K. W. Mort, and P. F. Yaggy, "Low-Speed Wind Tunnel Tests of A Large Scale Inflatable Structure Paraglider," *NASA TN D-2859*, 1965.
- [4] Ware, G.M., Hassell, J.L., "Wind-Tunnel Investigation of Ram-Air-Inflated All-Flexible Wings of Aspect Ratios 1.0 to 3.0". *NASA TM SX-1923, Langley Research Center*, Hampton, VA, 1969.
- [5] Goodrick, T.F., "Theoretical Study of the Longitudinal Stability of High-Performance Gliding Airdrop Systems". *AIAA Paper 75-1394, 5th Aerodynamic Decelerator Systems Conference*, 1975.
- [6] Goodrick, T.F., "Scale Effects on Performance of Ram Air Wings". *AIAA Paper 84-0783*, January 1984.
- [7] Brown, G.J., "Tethered Parafoil Test Technique". *AIAA 89-0903-CP*, January 1989.
- [8] C. Matos, R. Mahalingam, G. Ottinger, J. Klapper, R. Funk and N. Komerath, "Wind Tunnel Measurements of Parafoil Geometry and Aerodynamics", *36th AIAA Aerospace Sciences Meeting*, 1998.

[9] Gordon Strikert," Study on the relative motion of parafoil-load-systems", *Aerospace Science and Technology, Elsevier*, May 2004.

[10] M. Mashud and A.Umemura," Experimental Investigation of Aerodynamic Characteristics of a Paraglider Wing", *Transactions of JSASS* (submitted).